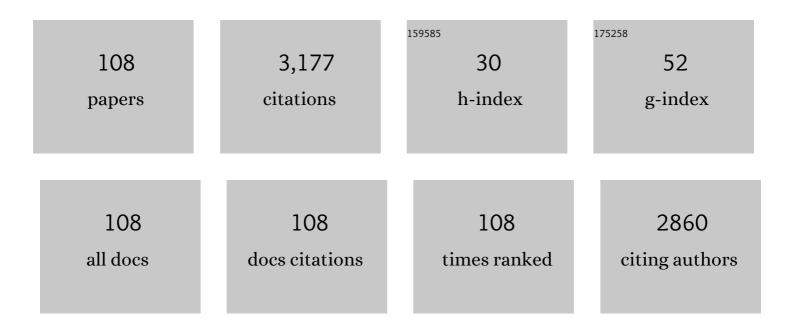


## List of Publications by Year in descending order

Source: https://exaly.com/author-pdf/1864535/publications.pdf Version: 2024-02-01



OLANC LL

#	Article	IF	CITATIONS
1	Layered Fe2(MoO4)3 assemblies with pseudocapacitive properties as advanced materials for high-performance sodium-ion capacitors. Chemical Engineering Journal, 2022, 427, 131481.	12.7	26
2	Transition metal catalysis in lithium-ion batteries studied by operando magnetometry. Chinese Journal of Catalysis, 2022, 43, 158-166.	14.0	8
3	Revealing the multiple cathodic and anodic involved charge storage mechanism in an FeSe <sub>2</sub> cathode for aluminium-ion batteries by <i>in situ</i> magnetometry. Energy and Environmental Science, 2022, 15, 311-319.	30.8	53
4	Perpendicular magnetization anisotropy induced dynamical coherence reduction in stripe domain film. Journal of Physics Condensed Matter, 2022, 34, 155802.	1.8	2
5	High Cycle Stability of Hybridized Co(OH)2 Nanomaterial Structures Synthesized by the Water Bath Method as Anodes for Lithium-Ion Batteries. Micromachines, 2022, 13, 149.	2.9	7
6	Electrochemical Role of Transition Metals in Sn–Fe Alloy Revealed by Operando Magnetometry. Chinese Physics Letters, 2022, 39, 028202.	3.3	1
7	Applications of nanogenerators for biomedical engineering and healthcare systems. InformaÄnÃ- Materiály, 2022, 4, .	17.3	45
8	Electrical control of ON–OFF magnetism and exchange bias via reversible ionic motion. Applied Physics Letters, 2022, 120, 082405.	3.3	3
9	Temperature prediction of lithiumâ€ion batteries based on electrochemical impedance spectrum: A review. International Journal of Energy Research, 2022, 46, 10372-10388.	4.5	51
10	Hollow CoS/C Structures for High-Performance Li, Na, K Ion Batteries. Frontiers in Chemistry, 2022, 10, 845742.	3.6	1
11	Revealing interfacial space charge storage of Li+/Na+/K+ by operando magnetometry. Science Bulletin, 2022, 67, 1145-1153.	9.0	23
12	Photo-induced non-volatile VO2 phase transition for neuromorphic ultraviolet sensors. Nature Communications, 2022, 13, 1729.	12.8	88
13	Evidence for dual anions co-insertion in a transition metal chalcogenide cathode material NiSe2 for high-performance rechargeable aluminum-ion batteries. Energy Storage Materials, 2022, 47, 336-344.	18.0	29
14	A comprehensive review on the state of charge estimation for lithiumâ€ion battery based on neural network. International Journal of Energy Research, 2022, 46, 5423-5440.	4.5	157
15	Mechanistic understanding of the charge storage processes in FeF <sub>2</sub> aggregates assembled with cylindrical nanoparticles as a cathode material for lithiumâ€ion batteries by in situ magnetometry. , 2022, 4, 1011-1020.		11
16	Annealing enhanced ferromagnetic resonance of thickness-dependent FeGa films. Applied Physics Letters, 2022, 120, 202402.	3.3	2
17	Unraveling the Evolution of Transition Metals during Li Alloying–Dealloying by In-Operando Magnetometry. Chemistry of Materials, 2022, 34, 5852-5859.	6.7	19
18	Dendrite-structured FeF2 consisting of closely linked nanoparticles as cathode for high-performance lithium-ion capacitors. Journal of Energy Chemistry, 2021, 55, 517-523.	12.9	25

#	Article	IF	CITATIONS
19	Co <sub>3</sub> S <sub>4</sub> Nanosheets on Carbon Cloth as Free-Standing Anode with Improved Pseudocapacitive Storage for High-Performance Li-Ion Batteries. Nano, 2021, 16, 2150007.	1.0	1
20	Waste Plastic Triboelectric Nanogenerators Using Recycled Plastic Bags for Power Generation. ACS Applied Materials & amp; Interfaces, 2021, 13, 400-410.	8.0	116
21	High electrochemical performance and structural stability of CoO nanosheets/CoO film as self-supported anodes for lithium-ion batteries. Ceramics International, 2021, 47, 5739-5746.	4.8	29
22	Extra storage capacity in transition metal oxide lithium-ion batteries revealed by in situ magnetometry. Nature Materials, 2021, 20, 76-83.	27.5	432
23	Construction of the POMOF@Polypyrrole Composite with Enhanced Ion Diffusion and Capacitive Contribution for High-Performance Lithium-Ion Batteries. ACS Applied Materials & Interfaces, 2021, 13, 6265-6275.	8.0	52
24	Orientation control of optical mode ferromagnetic resonance: From uniaxial to omni-directional. Applied Physics Letters, 2021, 118, .	3.3	3
25	Operando Magnetometry Probing the Charge Storage Mechanism of CoO Lithiumâ€ion Batteries. Advanced Materials, 2021, 33, e2006629.	21.0	80
26	Poly(vinylidene fluoride-trifluoroethylene)/cobalt ferrite composite films with a self-biased magnetoelectric effect for flexible AC magnetic sensors. Journal of Materials Science, 2021, 56, 9728-9740.	3.7	30
27	Multiple order spin-wave resonance in composition gradient sputtering FeCoB thin films. AIP Advances, 2021, 11, 075207.	1.3	0
28	Influence of surface pinning in the domain on the magnetization dynamics in permalloy striped domain films. Journal of Alloys and Compounds, 2021, 869, 159327.	5.5	7
29	Reacquainting the Electrochemical Conversion Mechanism of FeS <sub>2</sub> Sodium-Ion Batteries by Operando Magnetometry. Journal of the American Chemical Society, 2021, 143, 12800-12808.	13.7	69
30	Interfacial Control via Reversible Ionic Motion in Battery‣ike Magnetic Tunnel Junctions. Advanced Electronic Materials, 2021, 7, 2100512.	5.1	3
31	Coherent GHz lattice and magnetization excitations in thin epitaxial Ag/Fe/Cr/Fe films. Physical Review B, 2021, 104, .	3.2	1
32	Li-ionic control of magnetism through spin capacitance and conversion. Matter, 2021, 4, 3605-3620.	10.0	18
33	Fast potassium storage in porous CoV2O6 nanosphere@graphene oxide towards high-performance potassium-ion capacitors. Energy Storage Materials, 2021, 40, 250-258.	18.0	46
34	State-of-charge estimation and remaining useful life prediction of supercapacitors. Renewable and Sustainable Energy Reviews, 2021, 150, 111408.	16.4	113
35	Fe, N co-doped amorphous carbon as efficient electrode materials for fast and stable Na/K-storage. Electrochimica Acta, 2021, 396, 139265.	5.2	11
36	Evaluation of Metglas/polyvinylidene fluoride magnetoelectric bilayer composites for flexible in-plane resonant magnetic sensors. Journal Physics D: Applied Physics, 2021, 54, 095003.	2.8	8

#	Article	IF	CITATIONS
37	One-Pot Synthesized Amorphous Cobalt Sulfide With Enhanced Electrochemical Performance as Anodes for Lithium-Ion Batteries. Frontiers in Chemistry, 2021, 9, 818255.	3.6	3
38	Hydrothermal Preparation and High Electrochemical Performance of NiS Nanospheres as Anode for Lithium-Ion Batteries. Frontiers in Chemistry, 2021, 9, 812274.	3.6	2
39	Enhanced ferromagnetism and conductivity in epitaxial LaMnO3 thin films by oxygen-atmosphere annealing. Journal of Magnetism and Magnetic Materials, 2020, 499, 166317.	2.3	14
40	One-Pot Synthesis and High Electrochemical Performance of CuS/Cu1.8S Nanocomposites as Anodes for Lithium-Ion Batteries. Materials, 2020, 13, 3797.	2.9	13
41	Designing two-dimensional WS2 layered cathode for high-performance aluminum-ion batteries: From micro-assemblies to insertion mechanism. Nano Today, 2020, 32, 100870.	11.9	83
42	Nonaqueous Aluminum Ion Batteries: Recent Progress and Prospects. , 2020, 2, 887-904.		57
43	SnO2 nanoflower arrays on an amorphous buffer layer as binder-free electrodes for flexible lithium-ion batteries. Applied Surface Science, 2020, 527, 146910.	6.1	42
44	Laser Irradiation of Electrode Materials for Energy Storage and Conversion. Matter, 2020, 3, 95-126.	10.0	74
45	The abnormal damping behavior due to the combination between spin pumping and spin back flow in Ni80Fe20/Rut bilayers. Journal of Magnetism and Magnetic Materials, 2020, 502, 166495.	2.3	4
46	Intrinsic Defect-Rich Hierarchically Porous Carbon Architectures Enabling Enhanced Capture and Catalytic Conversion of Polysulfides. ACS Nano, 2020, 14, 6222-6231.	14.6	89
47	Reversible control of magnetization in Fe <sub>3</sub> O <sub>4</sub> nanoparticles by a supercapacitor. Journal of Physics Condensed Matter, 2020, 32, 334001.	1.8	15
48	Interfacial Engineering of Self-Supported SnO2Nanorod Arrays as Anode for Flexible Lithium-Ion Batteries. Journal of the Electrochemical Society, 2020, 167, 120515.	2.9	9
49	Spindle-like Fe3O4 nanoparticles for improving sensitivity and repeatability of giant magnetoresistance biosensors. Journal of Applied Physics, 2019, 126, .	2.5	14
50	Self-Supported Amorphous SnO <sub>2</sub> /TiO <sub>2</sub> Nanocomposite Films with Improved Electrochemical Performance for Lithium-Ion Batteries. Journal of the Electrochemical Society, 2019, 166, A3072-A3078.	2.9	45
51	Two-dimensionally porous cobalt sulfide nanosheets as a high-performance cathode for aluminum-ion batteries. Journal of Power Sources, 2019, 440, 227147.	7.8	33
52	Three-Dimensional Hierarchical Flowerlike FeP Wrapped with N-Doped Carbon Possessing Improved Li <sup>+</sup> Diffusion Kinetics and Cyclability for Lithium-Ion Batteries. ACS Applied Materials & Interfaces, 2019, 11, 39961-39969.	8.0	52
53	The effect of the particle size and magnetic moment of the Fe3O4 superparamagnetic beads on the sensitivity of biodetection. AIP Advances, 2019, 9, .	1.3	15
54	Synaptic memory devices from CoO/Nb:SrTiO <sub>3</sub> junction. Royal Society Open Science, 2019, 6, 181098.	2.4	12

#	Article	IF	CITATIONS
55	Multiferroic properties of aurivillius structure Bi4SmFeTi3O15 thin films. Journal of Materials Science: Materials in Electronics, 2019, 30, 9945-9954.	2.2	7
56	Ultrahigh Frequency and Anti-Interference Optical-Mode Resonance with Biquadratic Coupled FeCoB/Ru/FeCoB Trilayers. ACS Applied Materials & Interfaces, 2019, 11, 48230-48238.	8.0	10
57	Evolutions of acoustic and optical mode resonances in the spin reorientation Permalloy film. Journal of Applied Physics, 2019, 126, .	2.5	6
58	Influence of the phases structure on the acoustic and optical modes ferromagnetic resonance of FeNi stripe domain films. Journal of Magnetism and Magnetic Materials, 2019, 475, 103-107.	2.3	8
59	Stress-Enhanced Interlayer Exchange Coupling and Optical-Mode FMR Frequency in Self-Bias FeCoB/Ru/FeCoB Trilayers. ACS Applied Materials & Interfaces, 2018, 10, 8853-8859.	8.0	27
60	Improved Electrochemical Performance Based on Nanostructured SnS2@CoS2–rGO Composite Anode for Sodium-Ion Batteries. Nano-Micro Letters, 2018, 10, 46.	27.0	96
61	The influence of bias magnetization of nanoparticles on GMR sensor signal and sensitivity for the ultra-low concentration detection. Journal of Magnetism and Magnetic Materials, 2018, 453, 132-136.	2.3	12
62	Magnetization precession by short-wavelength magnon excitations and spin-transfer torque. Physical Review B, 2018, 97, .	3.2	5
63	Giant spontaneous exchange bias obtained by tuning magnetic compensation in samarium ferrite single crystals. Physical Chemistry Chemical Physics, 2018, 20, 3687-3693.	2.8	17
64	A Nanocrystalline Fe2O3 Film Anode Prepared by Pulsed Laser Deposition for Lithium-Ion Batteries. Nanoscale Research Letters, 2018, 13, 60.	5.7	23
65	Room-temperature magnetoelectric coupling in Bi4LaFeTi3O15 multiferroic films. Journal of Alloys and Compounds, 2018, 747, 1002-1007.	5.5	10
66	Thickness-dependent on the static magnetic properties and dynamic anisotropy of FeNi films with stripe domain structures. Journal Physics D: Applied Physics, 2018, 51, 025001.	2.8	17
67	3D Heterogeneous Co <sub>3</sub> O <sub>4</sub> @Co <sub>3</sub> S <sub>4</sub> Nanoarrays Grown on Ni Foam as a Binderâ€Free Electrode for Lithiumâ€ion Batteries. ChemElectroChem, 2018, 5, 309-315.	3.4	35
68	Constructing Three-Dimensional Porous Carbon Framework Embedded with FeSe <sub>2</sub> Nanoparticles as an Anode Material for Rechargeable Batteries. ACS Applied Materials & Interfaces, 2018, 10, 38862-38871.	8.0	69
69	Spin–transfer torque oscillator in magnetic tunneling junction with short–wavelength magnon excitation. AIP Advances, 2018, 8, .	1.3	1
70	Investigation on the structures and magnetic properties of carbon or nitrogen doped cobalt ferrite nanoparticles. Scientific Reports, 2018, 8, 7916.	3.3	15
71	Estimating the In-Plane Magnetic Anisotropy and Saturation Magnetization of Magnetic Films. IEEE Transactions on Magnetics, 2017, 53, 1-6.	2.1	5
72	Ultralow detection limit of giant magnetoresistance biosensor using \${mathrm{Fe}}_{3}{{m{O}}}_{4}\$ graphene composite nanoparticle label. Chinese Physics B, 2017, 26, 010701.	1.4	11

QIANG LI

#	Article	IF	CITATIONS
73	Optimization of NiFe 2 O 4 /rGO composite electrode for lithium-ion batteries. Applied Surface Science, 2017, 416, 308-317.	6.1	36
74	Stress-controllable microwave ferromagnetic performances of amorphous Fe56Co24B20 films prepared by pulsed laser deposition. Thin Solid Films, 2017, 636, 15-19.	1.8	4
75	CoO-Co nanocomposite anode with enhanced electrochemical performance for lithium-ion batteries. Electrochimica Acta, 2017, 224, 90-95.	5.2	56
76	Antimony Selenide Nanorods Decorated on Reduced Graphene Oxide with Excellent Electrochemical Properties for Li-Ion Batteries. Journal of the Electrochemical Society, 2017, 164, A2922-A2929.	2.9	30
77	High-temperature tunneling electroresistance in metal/ferroelectric/semiconductor tunnel junctions. Applied Physics Letters, 2017, 111, .	3.3	12
78	Tuning high frequency magnetic properties and damping of FeGa, FeGaN and FeGaB thin films. AIP Advances, 2017, 7, .	1.3	19
79	Electric Field Tuning Ferromagnetic Resonance Frequency Shift in Oblique Sputtered Fe42Co46Hf12/PZN-PT Multiferroic Heterostructures. IEEE Transactions on Magnetics, 2017, 53, 1-4.	2.1	2
80	Tunable Optical Mode Ferromagnetic Resonance in FeCoB/Ru/FeCoB Synthetic Antiferromagnetic Trilayers under Uniaxial Magnetic Anisotropy. Advanced Functional Materials, 2016, 26, 3738-3744.	14.9	75
81	Tunnel magnetoresistance in epitaxial (100)-oriented FeCo/LiF/FeCo magnetic tunnel junctions. Applied Physics Letters, 2016, 109, .	3.3	9
82	Electrical control of exchange bias via oxygen migration across CoO-ZnO nanocomposite barrier. Applied Physics Letters, 2016, 109, .	3.3	11
83	Applied magnetic field angle dependence of the static and dynamic magnetic properties in FeCo films during the deposition. Journal of Magnetism and Magnetic Materials, 2016, 416, 208-212.	2.3	15
84	Toward Onâ€andâ€Off Magnetism: Reversible Electrochemistry to Control Magnetic Phase Transitions in Spinel Ferrites. Advanced Functional Materials, 2016, 26, 7507-7515.	14.9	69
85	Investigation on the structure and dynamic magnetic properties of FeCo films with different thicknesses by vector network analyzer and electron spin resonance spectroscopy. Journal of Alloys and Compounds, 2016, 688, 917-922.	5.5	27
86	Engineering optical mode ferromagnetic resonance in FeCoB films with ultrathin Ru insertion. Scientific Reports, 2016, 6, 33349.	3.3	39
87	Ultra-wide detectable concentration range of GMR biosensors using Fe3O4 microspheres. Journal of Magnetism and Magnetic Materials, 2016, 417, 25-29.	2.3	27
88	Inverse tunnel magnetoresistance in epitaxial FeCo/MgO/Fe tunnel junctions patterned by in situ shadow-masks. Journal of Alloys and Compounds, 2016, 662, 79-83.	5.5	4
89	Detection of the Concentration of MnFe <sub>2</sub> O <sub>4</sub> Magnetic Microparticles Using Giant Magnetoresistance Sensors. IEEE Transactions on Magnetics, 2016, 52, 1-4.	2.1	16
90	Large rectification magnetoresistance in nonmagnetic Al/Ge/Al heterojunctions. Scientific Reports, 2015, 5, 14249.	3.3	18

#	Article	IF	CITATIONS
91	Self-bias ferromagnetic resonance and quasi magnetic isotropy of [FeCoB/MgO] <inf>6</inf> multilayers prepared by composition gradient sputtering. , 2015, , .		0
92	Self-Bias Ferromagnetic Resonance and Quasi-Magnetic Isotropy of (FeCoB/MgO) <sub>6</sub> Multilayers Prepared by Composition Gradient Sputtering. IEEE Transactions on Magnetics, 2015, 51, 1-3.	2.1	0
93	X-Ray Absorption Spectra and Self-Bias Ferromagnetic Resonance of FeCoB Films Prepared by Composition Gradient Sputtering. IEEE Transactions on Magnetics, 2015, 51, 1-4.	2.1	2
94	The Model for Linear Magnetoresistance of Two-Dimensional Metal-Semiconductor Composites with Interfacial Shells. Chinese Physics Letters, 2015, 32, 097501.	3.3	0
95	Large E-field tunability of magnetic anisotropy and ferromagnetic resonance frequency of co-sputtered Fe50Co50-B film. Journal of Applied Physics, 2015, 117, .	2.5	24
96	Electrical control of memristance and magnetoresistance in oxide magnetic tunnel junctions. Nanoscale, 2015, 7, 6334-6339.	5.6	21
97	Substantially enhancing ferromagnetic resonance frequency via superposition of composition gradient sputtering and magnetoelectric coupling in FeCoAlO/PZN–PT heterostructures. Journal of Alloys and Compounds, 2015, 642, 136-139.	5.5	6
98	Large inverse magnetoresistance induced by annealing effect in fully epitaxial FeCo/MgO/ Fe magnetic tunnel junctions. , 2015, , .		0
99	Multi-polar resistance switching and memory effect in copper phthalocyanine junctions. Chinese Physics B, 2014, 23, 058501.	1.4	1
100	Epitaxial growth of NaCl on Fe (100) and characterization of Fe/NaCl/Fe magnetic tunnel junctions. , 2014, , .		0
101	Electric field manipulation of nonvolatile magnetization in Au/NiO/Pt heterostructure with resistive switching effect. Applied Physics Letters, 2014, 105, .	3.3	35
102	Driving ferromagnetic resonance frequency of FeCoB/PZN-PT multiferroic heterostructures to Ku-band via two-step climbing: composition gradient sputtering and magnetoelectric coupling. Scientific Reports, 2014, 4, 7393.	3.3	55
103	Spin memristive magnetic tunnel junctions with CoO-ZnO nano composite barrier. Scientific Reports, 2014, 4, 3835.	3.3	21
104	Enhanced tunnel magnetoresistance in fully epitaxial ZnO:Co-based magnetic tunnel junctions with Mg-doped ZnO barrier. Applied Physics Letters, 2012, 100, .	3.3	11
105	Enhanced high-frequency electromagnetic properties of FeCoB–SiO2/SiO2 multilayered granular films. Physica B: Condensed Matter, 2012, 407, 1108-1113.	2.7	5
106	Effect of hydrogenation on transport and magnetic properties in homogeneous amorphous MnxGe1â´´x:H films. Journal of Applied Physics, 2011, 109, 083906.	2.5	6
107	Electric and Magnetic Field Tunable Rectification and Magnetoresistance in Fe <sub> <i>x</i> </sub> Ge <sub> 1â^ <i>x</i> </sub> /Ge Heterojunction Diodes. Chinese Physics Letters, 2011, 28, 107501.	3.3	1
108	Oxygen vacancies control of the electrical optical and magnetic properties of Fe0.05Ti0.95O2 epitaxial films. Chinese Physics B, 0, , .	1.4	0